JOURNAL OF NEUROCHEMISTRY | 2008 | 104 | 376–385 doi: 10.1111/j.1471-4159.2007.04977.x

Localization of the membrane-anchored MMP-regulator RECK at the neuromuscular junctions

Satoshi Kawashima,* Yukio Imamura,* Ediriweera P. S. Chandana,* Toru Noda,† Rei Takahashi,‡ Eijiro Adachi,§ Chiaki Takahashi*,¶ and Makoto Noda*

*Department of Molecular Oncology, Kyoto University Graduate School of Medicine, Sakyo-ku, Kyoto, Japan
†Department of Physical Therapy, Faculty of Nursing and Rehabilitation, Aino University, Ibaraki-shi, Osaka, Japan
‡Department of Pathology and Tumor Biology, Kyoto University Graduate School of Medicine, Sakyo-ku, Kyoto, Japan
§Department of Molecular Morphology, Kitasato University Graduate School of Medical Sciences, Sagamihara-shi, Kanagawa, Japan
¶The 21st Century Center of Excellence Program, Kyoto University Graduate School of Medicine, Sakyo-ku, Kyoto, Japan

Abstract

Nerve apposition on nicotinic acetylcholine receptor clusters and invagination of the post-synaptic membrane (i.e. secondary fold formation) occur by embryonic day 18.5 at the neuromuscular junctions (NMJs) in mouse skeletal muscles. Finding the molecules expressed at the NMJ at this stage of development may help elucidating how the strong linkage between a nerve terminal and a muscle fiber is established. Immunohistochemical analyses indicated that the membrane-anchored matrix metalloproteinase regulator RECK was enriched at the NMJ in adult skeletal muscles. Confocal and electron microscopy revealed the localization of RECK immunoreactivity in secondary folds and subsynaptic intracellular compartments in muscles. Time course studies indicated that RECK immunoreactivity becomes associated with the NMJ in the diaphragm at around embryonic day 18.5 and thereafter. These findings, together with known properties of RECK, support the hypothesis that RECK participates in NMJ formation and/or maintenance, possibly by protecting extracellular components, such as synaptic basal laminae, from proteolytic degradation.

Keywords: acetylcholine receptor, immunohistochemistry, matrix metalloproteinase, neuromuscular junctions, RECK, skeletal muscle.
J. Neurochem. (2008) **104**, 376–385.

The neuromuscular junction (NMJ) comprises portions of three types of cells – motor neuron, muscle fiber, and Schwann cell (Couteaux 1973; Ogata 1988; Engel 1994; Sanes and Lichtman 1999). The pre-synaptic membrane of the motor neuron contains dense patches called active zone where the neurotransmitter, acetylcholine (ACh), is released. The post-synaptic membrane of the muscle fiber is depressed into shallow gutters (primary gutters) beneath the nerve terminal and then further invaginated into ~1 μm-deep post-junctional folds (secondary folds) that open directly opposite active zones. Primary gutters and secondary folds are collectively called endplates. Nicotinic ACh receptor (AChR) is concentrated in the primary gutters, whereas voltage-gated sodium channels and dystrophin are concentrated in the secondary folds (Flucher and Daniels 1989; Bewick *et al.* 1992). α-bungarotoxin (BTX), a polypeptide snake toxin that binds tightly and specifically to AChR (Raftery 1973) has been used as a reliable probe for labeling AChR. Schwann cell processes cap the nerve terminal and help sustaining the environment necessary for proper neuronal activities. The synaptic basal lamina (BL) is a specialized form of extracellular matrix (ECM), which is sufficient to instruct synapses at the NMJ to re-form after denervation

Received April 4, 2007; revised manuscript received September 3, 2007; accepted September 6, 2007.

Address correspondence and reprint requests to Satoshi Kawashima, Department of Molecular Oncology, Kyoto University Graduate School of Medicine, Sakyo-ku, Kyoto 606-8501, Japan.
E-mail: mnoda@virus.kyoto-u.ac.jp

Abbreviations used: ACh, acetylcholine; AChR, nicotinic ACh receptor; BL, basal lamina; BTX, α-bungarotoxin; DB, dilution buffer; E18.5, embryonic day 18.5; ECM, extracellular matrix; GAPDH, glyceraldehyde-3-phosphate dehydrogenase; GPI, glycosylphosphatidylinositol; MMP, matrix metalloproteinase; MuSK, muscle-specific kinase; NMJ, neuromuscular junction; PBS, phosphate-buffered saline; PI-PLC, phosphatidylinositol-specific phospholipase C.

(Sanes *et al.* 1978; Burden *et al.* 1979). Laminin β2, also called s-laminin, is one of the molecules that form synaptic BL (Green *et al.* 1992; Patton *et al.* 1997). Laminin β2-deficient mice show aberrant synaptic development; the defects include lack of active zones, dispersal of synaptic vesicles, intrusion of Schwann cell processes into the synaptic cleft, and paucity of secondary folds (Noakes *et al.* 1995). The molecular mechanisms underlying the maintenance and functioning of these ECM structures at the NMJs, however, are still unclear and currently under intense investigations (Patton 2003). Nestin, an intermediate filament protein originally identified in neuroepithelial stem cells (Hockfield and McKay 1985), has also been identified in the subsynaptic region of the muscles (Carlsson *et al.* 1999), although its function at the NMJs is not fully understood.

Differentiation of three cell components precedes NMJ formation. Myogenesis is a multistep process involving determination, migration, alignment, and fusion of myoblasts to form myotubes that subsequently mature to give rise to muscle fibers (Buckingham *et al.* 2003). In vertebrates, motor neurons and Schwann cells arise from the ventral portion and the dorsal margin of the neural tube, respectively, and migrate toward muscles. Motor neurons reach muscles and make primitive contacts capable of rudimentary neurotransmission. As development proceeds, growth cones differentiate into nerve terminals. In mice, AChR-clustering in the central band of muscle occurs by embryonic day 14.5 (E14.5) through a nerve-independent mechanism (Lin *et al.* 2001; Yang *et al.* 2001). Many of these early AChR-clusters are not apposed by nerve terminals. By E16.5–18.5, all AChR clusters become apposed by nerve terminals (Lin *et al.* 2001). Secondary folds begin to form at this stage as well (Marques *et al.* 2000). Muscle-specific kinase (MuSK) and rapsyn are believed to play important roles in AChR-clustering (Burden *et al.* 1983; Sealock *et al.* 1984; Noakes *et al.* 1993; Hopf and Hoch 1998). Recent studies indicate that a membrane-associated adaptor protein, Dok-7, is also required for MuSK signaling and AChR clustering (Okada *et al.* 2006). A heparan sulfate proteoglycan, agrin, is thought to be required for the maturation and maintenance of AChR clusters, at least in part, by activating MuSK (Glass *et al.* 1996; Lin *et al.* 2001; Yang *et al.* 2001). Our knowledge on the molecules involved in NMJ formation, however, is still limited and needs to be enriched to understand how the strong linkage between nerve terminals and muscle fibers is established.

RECK was first isolated as a transformation suppressor gene by cDNA expression cloning in a mouse fibroblast cell line transformed by an activated *RAS* oncogene (Takahashi *et al.* 1998; Sasahara *et al.* 1999; Noda *et al.* 2003). *RECK* encodes a glycosylphosphatidylinositol (GPI)-anchored glycoprotein harboring three protease inhibitor-like domains, and its expression is reduced in many transformed and cancer cell lines. The extent of RECK down-regulation correlates with poor prognosis in cancer of various origins, such as the liver, pancreas, colorectum, and lung (Furumoto *et al.* 2001; Masui *et al.* 2003; Takenaka *et al.* 2004; Takeuchi *et al.* 2004). The RECK protein regulates at least three members of the matrix metalloproteinase (MMP) family, MMP-2, MMP-9, and MT1-MMP/MMP-14 (Takahashi *et al.* 1998; Oh *et al.* 2001), all known to play major roles in ECM degradation and cancer metastasis (Werb 1997; Egeblad and Werb 2002). Forced expression of RECK in cancer cell lines results in strong suppression of invasion, metastasis, and tumor angiogenesis (Takahashi *et al.* 1998; Oh *et al.* 2001). Mice lacking RECK die *in utero* with reduced integrity of blood vessels, the neural tube, and mesenchymal tissues (Oh *et al.* 2001). Although RECK expression is low during the early phase of myogenesis (before myoblast fusion), it becomes elevated in the later phase where myotubes mature (Echizenya *et al.* 2005). Likewise, during chondrogenesis, RECK expression is low in the early phase where cells form foci (cellular condensation), while it becomes up-regulated in the later phase where ECM accumulates in the resulting cartilaginous nodules (Kondo *et al.* 2007).

In this study, we analyzed the expression patterns of RECK in adult mice using immunohistochemical techniques and found strong RECK immunoreactivity at the NMJ. The RECK immunoreactivity becomes confined at the NMJ by ~E18.5 and is enriched in the secondary fold and intracellular compartment of the post-synaptic cells in adult mice. This association of RECK immunoreactivity with the NMJ coincides with complete juxtaposition of motor neurons to AChR clusters, suggesting a role for RECK in the formation and maturation of the NMJs.

Materials and methods

Tissue samples

Tissues were dissected from ICR mice of indicated stages, fixed in 1%*p*-formaldehyde in phosphate-buffered saline (PBS, pH 7.2) for 20 min at 4°C, rinsed briefly with PBS, incubated in 0.1 mol/L glycine in PBS for 1 h, incubated in Holts' Gum sucrose [30% sucrose, 1%'acacia' powder (Gum Arabic), 0.01% sodium azide in 0.1 mol/L phosphate buffer (pH 7.3)] overnight at 4°C, incubated in 50% OCT (Sakura, Tokyo, Japan) in Holts' Gum Sucrose overnight at 4°C, embedded in OCT (Sakura), frozen, and stored at −80°C until used. Tissues were sliced with a cryostat (HM500M; Leica, Tokyo, Japan). The sections were placed onto APS-coated glass slides (Matsunami, Tokyo, Japan). Denervation experiments were performed following the method of Vaittinen *et al.* (1999), except that the sciatic nerve was completely cut rather than squeezed. The animals were handled following Guideline for Animal Experiments of Kyoto University.

Immunohistochemistry

In the experiments shown in Fig. 2a–d and f, tissue sections were pre-incubated in dilution buffer [DB: 500 mmol/L NaCl, 0.01 mol/L

phosphate buffer (pH 7.2), 3% bovine serum albumin, 5% goat serum, 0.3% Triton, and 0.05% sodium azide] and incubated with primary rabbit antibodies in DB overnight at 4°C. After being rinsed in PBS, the sections were incubated with Alexa Fluor 555 goat anti-rabbit IgG (Invitogen, Tokyo, Japan), rinsed in PBS, treated with M.O.M.™ Mouse Ig Blocking Reagent (Vector, Burlingame, CA, USA), pre-incubated in DB, incubated with anti-RECK antibodies in DB, rinsed in PBS, and then incubated with Alexa Fluor 488 goat anti-mouse IgG (Invitrogen) in DB. The primary antibodies used were anti-synaptophysin 1 (rabbit polyclonal; Synaptic Systems, Göttingen, Germany), anti-S100 (rabbit polyclonal; DAKO, Tokyo, Japan), anti-laminin β2 (rabbit polyclonal; Santa Cruz Biotechnology Inc., Santa Cruz, CA, USA), anti-dystrophin (rabbit polyclonal; GeneTex, San Antonio, TX, USA), and anti-RECK (5B11D12, mouse monoclonal; Takahashi *et al.* 1998). In the experiments shown in Fig. 2e, tissue sections were pre-incubated in DB followed by incubation in anti-RECK antibody (IgG2a) pre-labeled with Zenon Alexa 488-conjugated anti-IgG2a Fab fragment (Invitrogen) plus monoclonal mouse anti-nestion antibody (IgG1) (Millipore, Temecula, CA, USA) pre-labeled with Alexa 555-conjugated anti-IgG1 Fab fragment (Invitrogen). After being rinsed in PBS, the sections were fixed in 4%*p*-formaldehyde in PBS. In the experiments shown in Figs 1, 3 and 5, tissue sections were first treated with M.O.M.™ Mouse Ig Blocking Reagent (Vector), pre-incubated in DB, incubated with anti-RECK antibodies in DB for 30 min at 25°C, rinsed in PBS, and then incubated in DB containing Alexa Fluor 488 goat anti-mouse IgG plus rhodamine-conjugated BTX (Invitrogen). All stained sections were finally washed in PBS and flat-mounted in Vectashield Mounting Medium with DAPI (Vector). Images were recorded using a fluorescent microscope (Zeiss, Tokyo, Japan) and/or confocal microscope (Olympus, Tokyo, Japan).

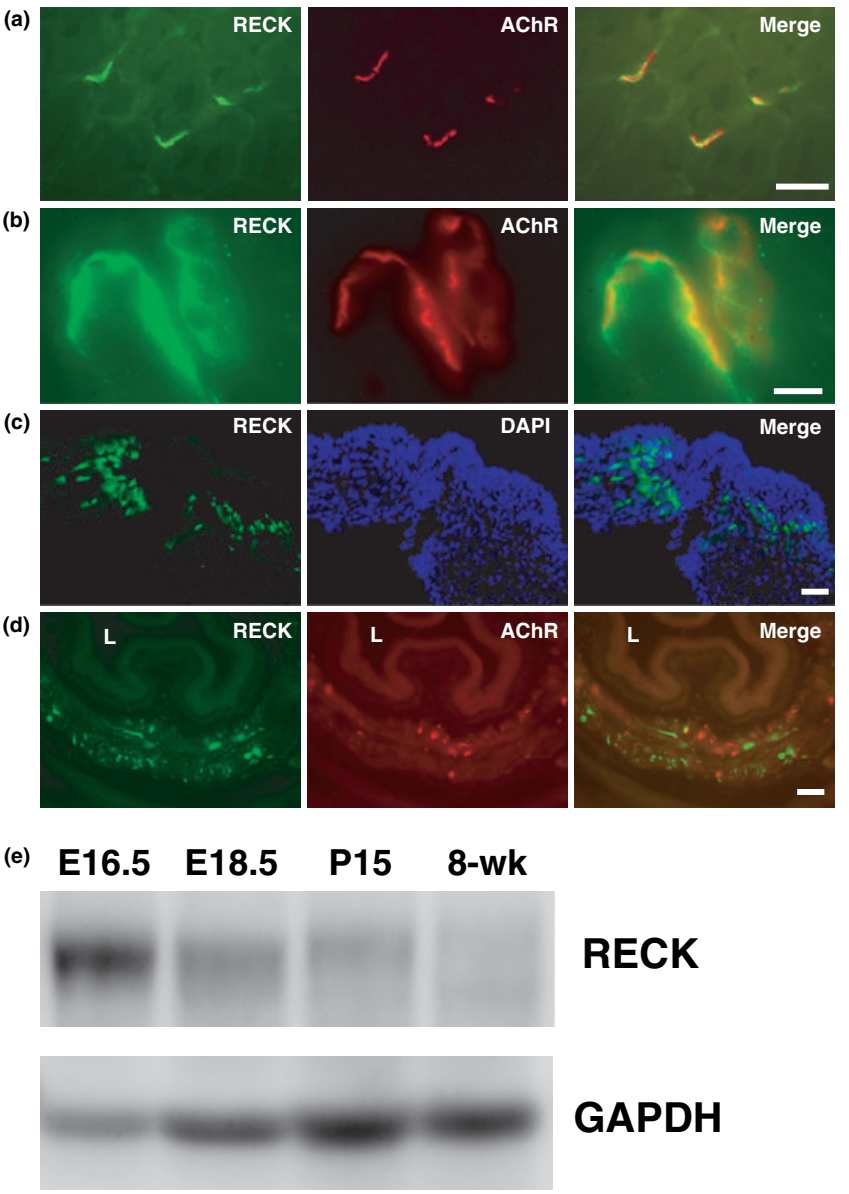

Fig. 1 Immunological detection of RECK in muscles. (a) A 6 μm-thick quadriceps section from 8-week-old mouse was double-stained with anti-RECK (left panel) and BTX (middle panel). The merged image (right panel) indicates tight association of RECK with AChR clusters. Subtype-matched non-specific IgG2a (negative control for anti-RECK staining) yielded no significant signals (not shown). (b) The NMJ in a diaphragm section stained by the same method. (c) Termini of muscle fibers in an E16.5 mouse diaphragm section double-stained with anti-RECK and DAPI (nuclei). (d) Esophagus in a section from P7 mouse double-stained with anti-RECK and BTX. Some smooth muscle cells show RECK immunoreactivity; association with AChR signals is rare. 'L' indicates esophagus lumen. (e) Immunoblot detection of the RECK protein in diaphragm lysates at indicated stages. Glyceraldehyde-3-phosphate dehydrogenase (GAPDH) was used as an internal control (bottom panel). Proportion of RECK protein to total proteins in skeletal muscles declines as development proceeds. Scale bar: (a) 50 μm, (b) 10 μm, (c) and (d) 50 μm.

Electron microscopy

Diaphragm of 8-week-old ICR mice was excised and fixed with Methyl-Carnoy's fixative (10% glacial acetic acid, 60% methanol, and 30% chloroform) for at least 3 h, immersed in methanol, and embedded in paraffin. Three micrometer-thick paraffin sections of these tissue blocks were cut with microtome and the sections were mounted on the glass slides (Matsunami). The sections were washed with PBS and stained by immunoperoxidase method with the anti-RECK antibody. The localization of RECK protein was visualized using EnVision+, Peroxidase, Mouse kit (DAKO). The NMJs with the positive reaction were selected using a light microscope and then processed for electron microscopic observations. After diaminobenzoate reaction of the immunohistochemical step, the sections were post-fixed in 1% OsO_4 in 25 mmol/L PIPES buffer, pH 7.4 for 60 min, dehydrated in a series of graded ethanols and propylene oxide. The sections were finally covered with the inverted BEEM-capsules filled with the Epon-equivalent resin embedding medium (Luveak®-812; Nacalai Tesque, Kyoto, Japan), and cured in 80°C for 24 h. After polymerization, the tissue sections on the glass slides were transferred to polymerized block and the ultrathin sections of RECK-positive NMJ were cut and observed under JEM 1200EX (JEOL, Tokyo, Japan) with the accelerating voltage of 80 kV.

Immunoblot assay

Diaphragms from ICR mice of different developmental stage (E16.5∼8-week old) were dissected, ground in liquid nitrogen, and lysed in 50 mmol/L Tris–Cl (pH 6.8), 1 mmol/L EDTA, 1% sodium dodecyl sulfate, and protease inhibitor cocktail (Nakalai, Kyoto, Japan). The homogenates were cleared by centrifugation at 12 000 *g* for 20 min, and their protein concentration was determined. The sample (40 μg protein) was separated by sodium dodecyl sulfate–polyacrylamide gel electrophoresis (10% acrylamide), followed by immunoblot detection using mouse monoclonal and goat polyclonal antibody against RECK (5B11D12) and glyceraldehyde-3-phosphate dehydrogenase (Santa Cruz Biotechnology Inc.), respectively. For visualization, the Immobilon Western Blot Kit (Millipore) was used with horseradish peroxidase-conjugated anti-mouse (for RECK) or anti-goat IgG-F(ab′)2 antibodies (for glyceraldehyde-3-phosphate dehydrogenase).

Results

RECK immunoreactivity at the NMJs

To find clues to the functions of RECK *in vivo*, we stained slices of various tissues at various stages with an anti-RECK monoclonal antibody, 5B11D12. We found prominent signals at small regions in skeletal muscles (e.g. the quadriceps and diaphragm) in 8-week-old mice; most signals were associated with the AChR clusters visualized by BTX-labeling (Fig. 1a and b), suggesting accumulation of RECK-immunoreactivity at the NMJs. Strong RECK-immunoreactivity was also found at the termini of muscle fibers at E16.5 (Fig. 1c) and some smooth muscle cells surrounding esophagus at postnatal day 7 (Fig. 1d). Our previous study indicated that in earlier stages of skeletal muscle development (E13.5), RECK immunoreactivity was found on the entire surface of myotubes (Echizenya *et al.* 2005). In contrast, strong RECK immunoreactivity is confined at the NMJs in adult skeletal muscles. Immunoblot assay with whole diaphragm lysates indicated that the amount of RECK (approximate molecular mass: 110 kDa) per total cellular protein was gradually declined after E16 (Fig. 1e).

Subdomain distribution of RECK immunoreactivity at the NMJ

We next tried to define the location of abundant RECK immunoreactivity more precisely by examining the diaphragm sections doubly labeled for RECK and another cell type marker by confocal microscopy (Fig. 2). First, a large part of the strong RECK immunoreactivity did not coincide with S100 signals nor synaptophysin 1 signals (Fig. 2a and b), making it unlikely that RECK is abundant in Schwann cells or motor nerve terminals. Second, under these conditions, RECK immunoreactivity did not exactly coincide with AChR signals and partially overlapped with dystrophin signals (Fig. 2c and d), suggesting that RECK is abundant in secondary folds rather than primary gutters. Third, RECK immunoreactivity largely coincided with nestin signals (Fig. 2e) known to be accumulated between the lower portions of secondary folds and the subsynaptic nuclei in the muscle (Carlsson *et al.* 1999). Fourth, the RECK immunoreactivity largely overlapped with laminin β2 signals, known to associate with synaptic BLs (Fig. 2f). These findings suggest that RECK immunoreactivity is associated mainly with secondary folds and subsynaptic area in the muscle.

RECK is a GPI-anchored protein and has been shown, using cultured cells, to be released into culture supernatant upon treatment with phosphatidylinositol-specific phospholipase C (PI-PLC) (Takahashi *et al.* 1998). Treatment of diaphragm sections with PI-PLC prior to immunostaining resulted in greatly reduced RECK immunoreactivity (Fig. 3a). We also studied the behaviors of RECK immunoreactivity at the tibialis anterior muscle NMJs after incision of sciatic nerve. Successful denervation was confirmed by ataxic gait (not shown) and decline in the number of synaptophysin 1-positive AChR clusters (∼80% at day 3) (Fig. 3b and c). At this time point, persistent association of RECK immunoreactivity with AChR clusters (Fig. 3d) as well as laminin β2 signals (Fig. 3e) was observed, strengthening our hypothesis that RECK immunoreactivity is associated with post-synaptic membrane.

Electron microscopic examination of RECK immunoreactivity at the NMJ

To further define the RECK localization at the NMJs, we performed immunoelectron microscopy (Fig. 4). Strong RECK immunoreactivity is found around the bottom of secondary folds (Fig. 4, arrows) and intracellular compart-

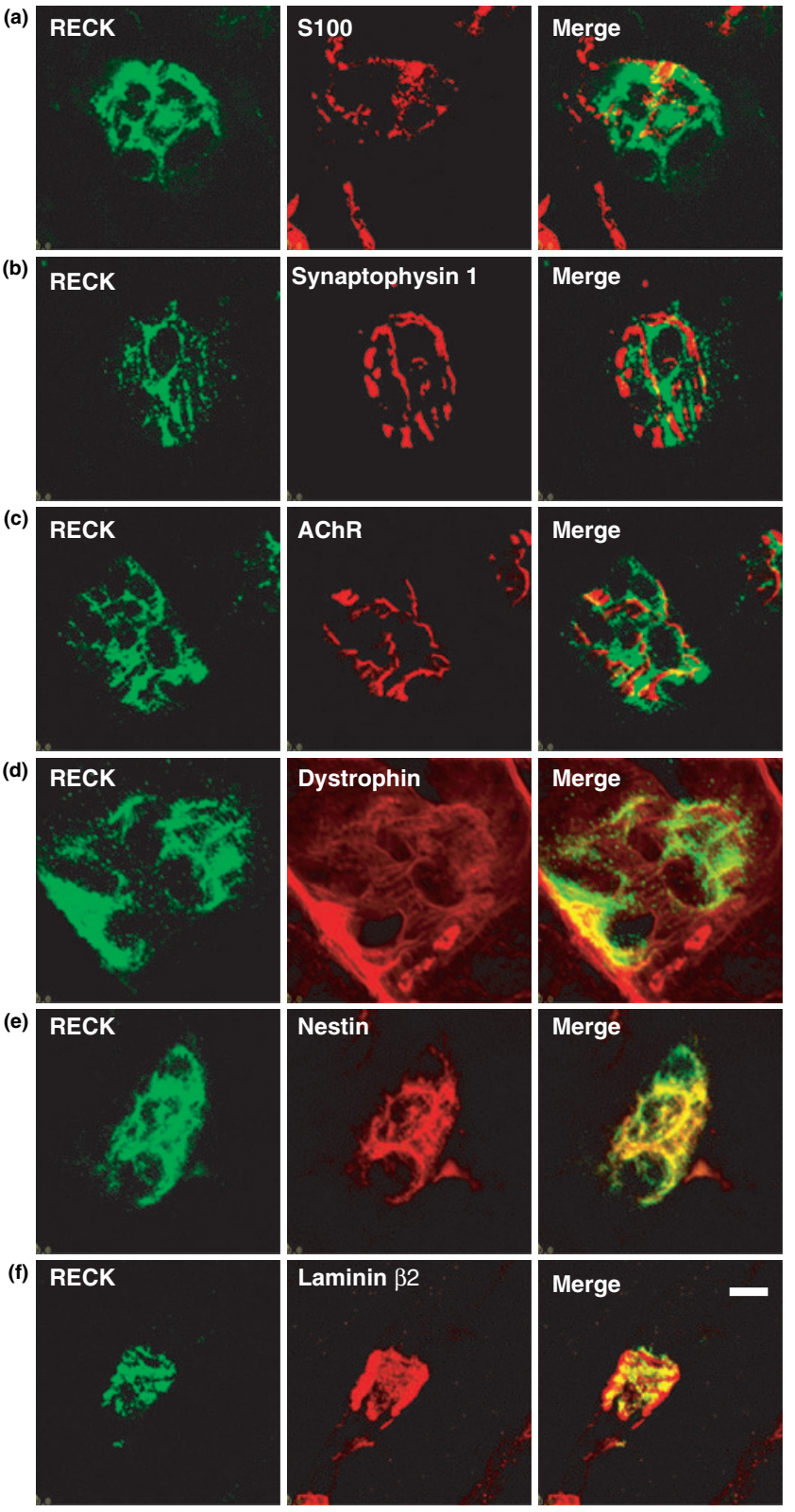

Fig. 2 Topological relationships between RECK immunoreactivity and NMJ subdomain markers. Sections (8-μm thick) of the diaphragms from 8-week-old mice were double-stained with anti-RECK (green) and an NMJ subdomain marker (red) and examined by confocal microscopy. The subdomain markers used: (a) S100 [Schwann cells], (b) synaptophysin 1 [motor nerve terminals], (c) BTX [primary gutters], (d) dystrophin [secondary folds], (e) nestin, and (f) laminin β2 [synaptic BL]. Scale bar: 5 μm.

ments beneath the synapse. RECK immunoreactivity is low, if any, around the neuron/Schwann cell compartments (Fig. 4, the area between M1 and M2) and the other parts of the muscle (Fig. 4, M2). These findings (summarized in Fig. 4d) establish the abundant, post-synaptic localization of RECK immunoreactivity at the NMJ.

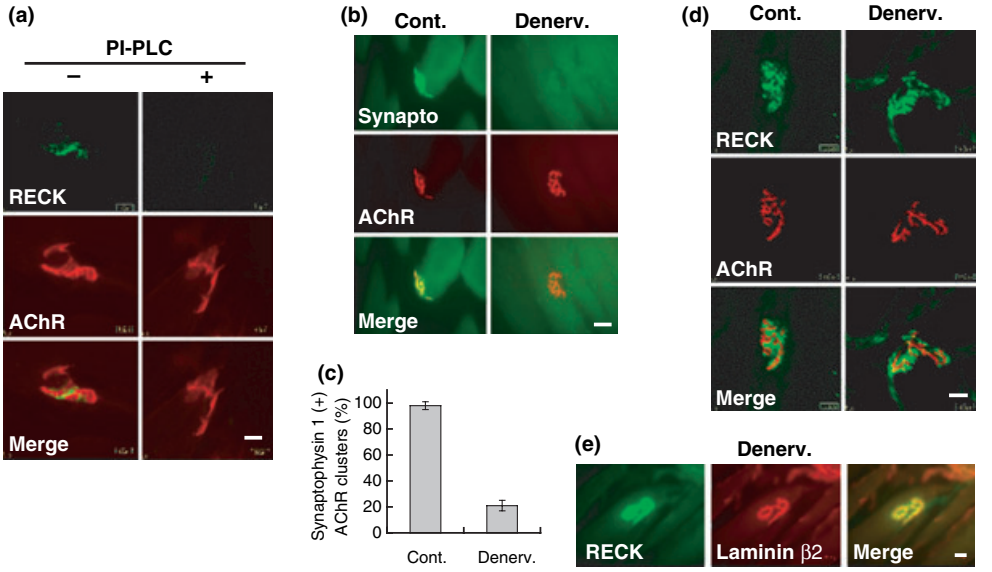

Fig. 3 Effects of PI-PLC-treatment and denervation on the RECK immunoreactivity. (a) Diaphragm slices were incubated in the absence (–) or presence (+) of PI-PLC (1 mU/μL in PBS) at 37°C for 1 h before staining with anti-RECK (green) and BTX (red). Representative images are shown. Note the reduced RECK immunoreactivity after PI-PLC treatment. (b) Thigh femur muscle of the left hind limb of adult mouse was denervated by cutting deep peroneal nerve. Three days later, the tibialis anterior muscle of the denervated left hind limb (Denerv.) and the control right hind limb (Cont.) were resected and their slices were doubly stained for synaptophysin 1 (green) and AChR (red). Note the absence of synaptophysin 1 signals associated with AChR signals after denervation. (c) Proportion of synaptophysin 1-positive AChR clusters in the slices of control ($n = 4$) and denervated ($n = 3$) muscles (mean ± SE, $p = 1.76 \times 10^{-4}$, Student's *t*-test). (d) Slices of control and denervated muscles were doubly stained for RECK (green) and AChR (red). Representative images are shown. The RECK immunoreactivity remains associated with AChR clusters after denervation. (e) Slices of denervated muscles were doubly stained for RECK and laminin β2. Representative images are shown. Scale bar: (a) 5 μm, (b) 20 μm, (d) 10 μm, (e) 20 μm.

Time course of the association of RECK immunoreactivity with the NMJs during development

We also noticed, however, that the association of RECK immunoreactivity to the AChR clusters is not found in the diaphragm of mouse embryos at E14.5 (Fig. 5a). To extend this finding, we performed a systematic analysis of the proportion of AChR clusters associated with RECK immunoreactivity at different developmental stages (Fig. 5b–g). At E16.5, only a small fraction of AChR clusters were positive for RECK immunoreactivity (Fig. 5b and g). In contrast, majority (≥70%) of the AChR clusters were positive for RECK immunoreactivity at E18.5 and thereafter (Fig. 5c–f and g). Thus, association of RECK immunoreactivity to the NMJs seem to occur in a relatively confined period (E16.5–18.5) during development. We also found that the RECK immunoreactivity at the NMJs becomes slightly diffuse during certain period after birth, e.g. postnatal day 7 and 15 (Fig. 5d and e).

Discussion

In this study, we detected strong RECK immunoreactivity at the NMJs in skeletal muscles (e.g. the quadriceps and diaphragm) in adult mice. This finding prompted us to analyze the spatial and temporal expression patterns of RECK immunoreactivity in the diaphragm. We chose to concentrate on the diaphragm, as (i) it contains skeletal muscles abundantly, (ii) it is amenable to immunohistochemical analyses, and (iii) it has previously been used for analyzing NMJ development by many researchers. Confocal and electron-microscopic observation of the diaphragm from 8-week-old mice revealed the localization of RECK immunoreactivity around the secondary folds of mature NMJs and some post-synaptic, intracellular compartments (see Fig. 4c for schematic representation). It has been reported that the secondary fold is abundant in neural cell adhesion molecule, voltage-gated sodium channel, ankyrin, dystrobrevin-2, dystrophin, syntrophin α1 and β1, and erbB2/4 (Sanes and Lichtman 1999; Trinidad *et al.* 2000). Indeed, we found overlapped localization of dystrophin and RECK immunoreactivity in this study (Fig. 2d).

The present study relies on the monoclonal anti-RECK antibody, 5B11D12, which is the only reagent currently available for labeling RECK in mouse tissues. Specificity of this antibody has been tested in several ways: i.e. (i) immunoblot comparisons between vector-transfected and RECK-transfected HT1080 cells (Takahashi *et al.* 1998), (ii) immunoblot comparisons between embryo fibroblasts derived from wild type and RECK-null mice (Oh *et al.* 2001), and (iii) immunohistochemical comparison between wild

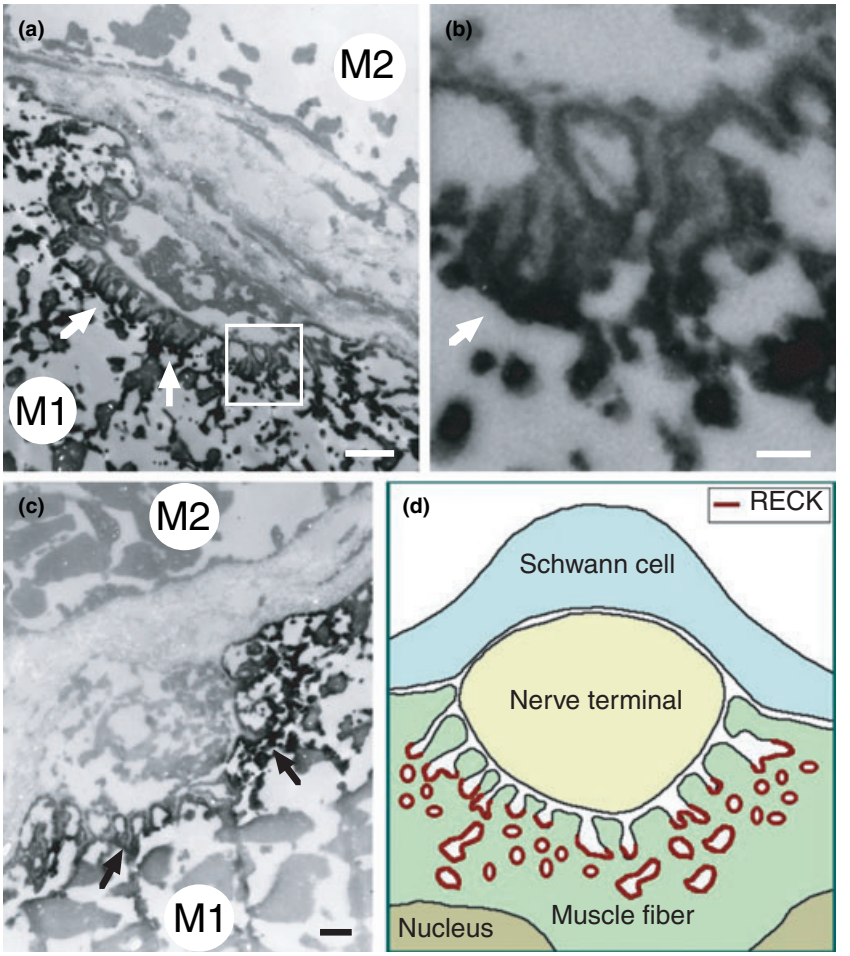

Fig. 4 Detection of RECK immunoreactivity at the NMJ by electron microscopy. Two representative images (a, c) of the NMJs in the 8-week-old mouse diaphragm immunolabeled with anti-RECK antibodies and detected as diaminobenzoate reaction products. A magnified view of one area of (a) (white rectangle) is shown in (b). The electron dense reaction products are found at the depths of secondary folds (arrows) and intracellular compartments in the muscle (M1). The reaction products are not found in the adjacent muscle fiber (M2). Scale bar: (a) 1 μm, (b) 200 nm, (c) 500 nm and (d) Summary of the findings.

type and RECK-null mouse embryos (Oh *et al.* 2001). Our finding in this study that pre-treatment of tissues with PI-PLC greatly reduce the immunoreactivity (Fig. 3a) further support our presumption that the immunoreactivity we detected at the NMJ represents GPI-anchored RECK protein.

Identity of the round or oval structures positive for RECK-immunoreactivity found in the subsynaptic region (Fig. 4b) is presently unclear. Some of them may represent extended secondary folds. Some others may represent membrane vesicles containing nascent RECK molecules on the way to the plasma membrane or internalized by endocytosis. A proposed role for the NMJ-associated nestin is to help anchoring subsynaptic nuclei to the endplate region (Carlsson *et al.* 1999), and such a cytoskeleton may be related to a mechanism which selectively regulates these nuclei to provide mRNA for the synthesis of the unique proteins localized at the endplates (Traub 1995). The observed colocalization between RECK and nestin may indicate that RECK is one of such endplate-associated proteins. Alternatively, RECK may protect such endplate-associated proteins, both *en route* and on cell surface, from protease-mediated degradation. On the other hand, some GPI-anchored proteins are known to be delivered to recycling endosomes via a Cdc42-regulated, clathrin-independent pinocytic pathway (Sabharanjak *et al.* 2002). Our recent study using fibrosarcoma cells in culture have indicated that RECK may recruit some membrane-associated proteins to an intracellular compartment that accelerates degradation of these proteins (Miki *et al.* 2007). Thus, these and other possibilities need to be tested to understand the roles of subsynaptic, RECK-positive intracellular structures.

Our previous study indicated that abundant RECK immunoreactivity was found on the surface (especially near the termini) of myofibers at E13.5 (Echizenya *et al.* 2005). Similar pattern of RECK immunoreactivity could be seen in diaphragm at E14.5–E16.5 (Fig. 4a and b; the green puncta most probably represent termini of muscle fibers). Strong RECK immunoreactivity, however, become confined to the NMJs during skeletal muscle development (Fig. 5). Hence, RECK may be required on the whole muscle surface during myogenesis and then become important for the formation and/or functions of the NMJ after certain developmental stage. Our previous study implicate MRF4 in RECK gene activation, especially in the terminal regions of muscle fibers

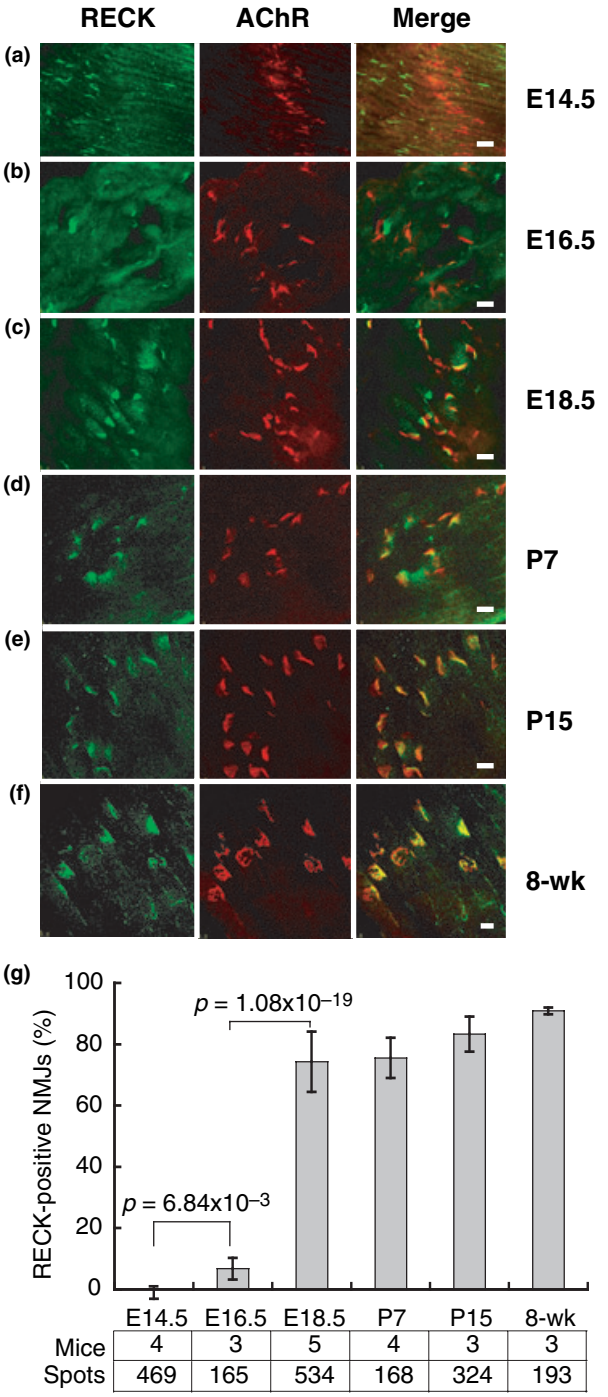

Fig. 5 Time course of the association of RECK immunoreactivity with the NMJ. Sections (20-μm thick) of the diaphragm from mice at indicated stages were double-stained with anti-RECK (green) and BTX (red) and examined with a fluorescence microscope (a) or a confocal microscope (b–f). At E14.5 and E16.5, few 5B-reactive spots overlap with BTX-positive spots. At E18.5 and thereafter, however, majority of 5B-reactive spots are found in the close vicinity of BTX-signals. Scale bar: (a) 50 μm and (b–f) 20 μm. (g) Proportion of 5B-reactive spots among BTX-positive spots at indicated developmental stage (mean ± SE among individual animals; *p*, Student's *t*-test). The numbers of animals used and the total number of spots examined are indicated below the bar.

(Echizenya *et al.* 2005). On the other hand, neuromuscular interactions, probably through signaling molecules such as neuregulin, agrin, and ACh itself, has been implicated in synaptic nuclei-specific gene activation during NMJ maturation (Burden 2002). It would be interesting to test whether RECK expression is influenced, or becomes susceptible to the action of, these signaling molecules during NMJ maturation.

The NMJs associated with RECK immunoreactivity increased during embryogenesis and reached plateau at around E18.5 (~70%) (Fig. 5). Previous studies indicate that by this stage, all AChR clusters in the central band of muscle become apposed by nerve terminals (Lin *et al.* 2001) and secondary folds begin to form (Marques *et al.* 2000). RECK may therefore play some roles in these events (see below). The nature of the remaining 30% of the NMJs devoid of RECK immunoreactivity is unclear at the moment, but they may represent possible heterogeneity among NMJs (Brunelli *et al.* 2005).

What would be the roles for RECK in developing NMJs? Bloch *et al.* (1986) reported that AChR clusters become resistant to dispersal by collagenase around the perinatal stage. As RECK is known to regulate some MMPs exhibiting collagenase activity, RECK may contribute to this development-associated consolidation of AChR clusters. RECK may also be required for the stabilization of the synaptic BL, a target of MMPs, that links pre- and post-synaptic membranes. Laminin β2 is known to contribute to the formation of fully functional NMJs by affecting all three types of cells that form the NMJ (Noakes *et al.* 1995). It is therefore intriguing to speculate that RECK may protect laminin β2 from proteolysis, thereby assisting NMJ formation. RECK may also protect other membrane-associated proteins from MMP-mediated degradation; interesting candidates are integrins, as mice lacking another MMP-regulator, TIMP-2, show reduced β1 integrin in fast-twitch muscles and display signs of muscle weakness probably because of destabilized ECM–cytoskeletal interaction (Lluri *et al.* 2006). Alternatively, RECK may play more active roles in NMJ formation. For instance, secondary fold formation involves extensive invagination of post-synaptic membrane as well as associated BL, and this process is likely to required active ECM-remodeling; in fact, excessive secondary fold formation has been observed in MMP-3-deficient mice (VanSaun *et al.* 2003). RECK may well be involved in the regulation of such process.

Persistent expression of RECK at the NMJs in adult mice may suggest the role for RECK in the maintenance and/or functioning of NMJs. *RECK* is a single gene conserved from fly to mammals. Interestingly, the nematode genome lacks

RECK ortholog, and agrin is at a high rank among the proteins that share partial homology to RECK. RECK and agrin may therefore share a common ancestry and, possibly, play related roles. Agrin is believed to be important for the maintenance of AChR clusters in the primary gutter (Lin *et al.* 2001; Yang *et al.* 2001). Likewise, RECK may be important for the maintenance of certain molecular complexes (e.g. dystrophin–dystroglycan complex, $\alpha_7\beta_1$ integrin, etc.) in the secondary fold.

The present study suggests the possible roles for RECK in the formation, maintenance, and/or functioning of NMJs. Several lines of experiments to test these possibilities can be proposed. First, patterns of RECK expression in mice defective in molecules important for NMJ formation, such as HB9, agrin, MuSK, rapsyn, Dok-7, etc., need to be analyzed. Second, as mice lacking *RECK* die around E10.5, other methods of gene silencing (e.g. siRNA, Cre-loxP-mediated conditional gene inactivation, etc) may be useful. Third, electrophysiological techniques may also be useful in addressing the functional implication of RECK-deficiency. Through these studies, we may be able to answer the questions of how RECK influences NMJ development and why RECK needs to be up-regulated around E18.5 and kept high thereafter at the NMJ.

Acknowledgements

We thank Aki Nishimoto, Takashi Kawai, Hai-Ou Gu, and Mari Kojima for technical assistance, Aki Miyazaki for secretarial assistance, and Drs Kuo-Fen Lee and Noriaki Noma for technical advice and discussion. This work was supported by JSPS Grant-in-Aid for Creative Scientific Research and MEXT Grant-in-Aid on Priority Areas.

References

Bewick G. S., Nicholson L. V., Young C., O'Donnell E. and Slater C. R. (1992) Different distributions of dystrophin and related proteins at nerve-muscle junctions. *Neuroreport* **3**, 857–860.

Bloch R. J., Steinbach J. H., Merlie J. P. and Heinemann S. (1986) Collagenase digestion alters the organization and turnover of junctional acetylcholine receptors. *Neurosci. Lett.* **66**, 113–119.

Brunelli G., Spano P., Barlati S., Guarneri B., Barbon A., Bresciani R. and Pizzi M. (2005) Glutamatergic reinnervation through peripheral nerve graft dictates assembly of glutamatergic synapses at rat skeletal muscle. *Proc. Natl Acad. Sci. USA* **102**, 8752–8757.

Buckingham M., Bajard L., Chang T., Daubas P., Hadchouel J., Meilhac S., Montarras D., Rocancourt D. and Relaix F. (2003) The formation of skeletal muscle: from somite to limb. *J. Anat.* **202**, 59–68.

Burden S. J. (2002) Building the vertebrate neuromusclular synapse. *J. Neurobiol.* **53**, 501–511.

Burden S. J., Sargent P. B. and McMahan U. J. (1979) Acetylcholine receptors in regenerating muscle accumulate at original synaptic sites in the absence of the nerve. *J. Cell Biol.* **82**, 412–425.

Burden S. J., DePalma R. L. and Gottesman G. S. (1983) Crosslinking of proteins in acetylcholine receptor-rich membranes: association between the beta-subunit and the 43 kd subsynaptic protein. *Cell* **35**, 687–692.

Carlsson L, Li Z, Paulin D and Thornell LE. (1999) Nestin is expressed during development and in myotendinous and neuromuscular junctions in wild type and desmin knock-out mice. *Exp. Cell Res.* **251**, 213–223.

Couteaux R. (1973) Motor endplate structure, in *Structure and Function of Muscle* (Bourne G. H., ed.), Vol. 2, pp. 483–530. Academic, New York.

Echizenya M., Kondo S., Takahashi R., Oh J., Kawashima S., Kitayama H., Takahashi C. and Noda M. (2005) The membrane-anchored MMP-regulator RECK is a target of myogenic regulatory factors. *Oncogene* **24**, 5850–5857.

Egeblad M. and Werb Z. (2002) New functions for the matrix metalloproteinases in cancer progression. *Nat. Rev. Cancer* **2**, 161–174.

Engel A. G. (1994) The neuromuscular junction, in *Myology: Basic and Clinical* (Engel A. G. and Franzini-Armstrong C., eds.), Vol. 1, pp. 261–302. McGraw-Hill, New York.

Flucher B. E. and Daniels M. P. (1989) Distribution of Na+ channels and ankyrin in neuromuscular junctions is complementary to that of acetylcholine receptors and the 43 kd protein. *Neuron* **3**, 163–175.

Furumoto K., Arii S., Mori A. *et al.* (2001) RECK gene expression in hepatocellular carcinoma: correlation with invasion-related clinicopathological factors and its clinical significance. Reverse-inducing – cysteine-rich protein with Kazal motifs. *Hepatology* **33**, 189–195.

Glass D. J., Bowen D. C., Stitt T. N. *et al.* (1996) Agrin acts via a MuSK receptor complex. *Cell* **85**, 513–523.

Green T. L., Hunter D. D., Chan W, Merlie J. P and Sanes J. R. (1992) Synthesis and assembly of the synaptic cleft protein S-laminin by cultured cells. *J. Biol. Chem.* **267**, 2014–2022.

Hockfield S and McKay R. D. (1985) Identification of major cell classes in the developing mammalian nervous system. *J. Neurosci.* **5**, 3310–3328.

Hopf C. and Hoch W. (1998) Dimerization of the muscle-specific kinase induces tyrosine phosphorylation of acetylcholine receptors and their aggregation on the surface of myotubes. *J. Biol. Chem.* **273**, 6467–6473.

Kondo S., Shukunami C., Morioka Y. *et al.* (2007) Dual effects of the membrane-anchored MMP regulator RECK on chondrogenic differentiation of ATDC5 cells. *J. Cell Sci.* **120**, 849–857.

Lin W., Burgess R. W., Dominguez B., Pfaff S. L, Sanes J. R and Lee K. F. (2001) Distinct roles of nerve and muscle in postsynaptic differentiation of the neuromuscular synapse. *Nature* **410**, 1057–1064.

Lluri G., Langlois G. D., McClellan B., Soloway P. D. and Jaworski D. M. (2006) Tissue inhibitor of metalloproteinase-2 (TIMP-2) regulates neuromuscular junction development via a beta1 integrin-mediated mechanism. *J. Neurobiol.* **66**, 1365–1377.

Marques M. J., Conchello J. A. and Lichtman J. W. (2000) From plaque to pretzel: fold formation and acetylcholine receptor loss at the developing neuromuscular junction. *J. Neurosci.* **20**, 3663–3675.

Masui T., Doi R., Koshiba T. *et al.* (2003) RECK expression in pancreatic cancer: its correlation with lower invasiveness and better prognosis. *Clin Cancer Res.* **9**, 1779–1784.

Miki T., Takegami Y., Okawa K., Muraguchi T., Noda M. and Takahashi C. (2007) The reversion-inducing cystein-rich protein with Kazal motifs (RECK) interacts with membrane type 1 matrix metalloproteinase (MT1-MMP) and C13/aminopeptidase N (APN) and modulates their endocytic pathways. *J. Biol. Chem.* **282**, 12341–12352.

Noakes P. G., Phillips W. D., Hanley T. A., Sanes J. R. and Merlie J. P. (1993) 43K protein and acetylcholine receptors colocalize during the initial stages of neuromuscular synapse formation in vivo. *Dev. Biol.* **155**, 275–280.

Noakes P. G., Gautam M., Mudd J., Sanes J. R. and Merlie J. P. (1995) Aberrant differentiation of neuromuscular junctions in mice lacking s-laminin/laminin beta 2. *Nature* **374**, 258–262.

Noda M., Oh J., Takahashi R., Kondo S., Kitayama H. and Takahashi C. (2003) RECK: a novel suppressor of malignancy linking oncogenic signaling to extracellular matrix remodeling. *Cancer Metastasis Rev.* **22**, 167–175.

Ogata T. (1988) Structure of motor endplates in the different fiber types of vertebrate skeletal muscles. *Arch. Histol. Cytol.* **51**, 385–424.

Oh J., Takahashi R., Kondo S. *et al.* (2001) The membrane-anchored MMP inhibitor RECK is a key regulator of extracellular matrix integrity and angiogenesis. *Cell* **107**, 789–800.

Okada K., Inoue A., Okada M. *et al.* (2006) The muscle protein Dok-7 is essential for neuromuscular synaptogenesis. *Science* **312**, 1802–1805.

Patton B. L. (2003) Basal lamina and the organization of neuromuscular synapses. *J. Neurocytol.* **32**, 883–903.

Patton B. L, Miner J. H, Chiu A. Y and Sanes J. R. (1997) Distribution and function of laminins in the neuromuscular system of developing, adult, and mutant mice. *J. Cell Biol.* **139**, 1507–1521.

Raftery M. A. (1973) Isolation of acetylcholine receptor – bungarotoxin complexes from Torpedo californica electroplax. *Arch. Biochem. Biophys.* **154**, 270–276.

Sabharanjak S., Sharma P., Parton RG. and Mayor S. (2002) GPI-anchored proteins are delivered to recycling endosomes via a distinct cdc42-regulated, clathrin-independent pinocytic pathway. *Dev. Cell* **2**, 411–423.

Sanes J. R. and Lichtman J. W. (1999) Development of the vertebrate neuromuscular junction. *Annu. Rev. Neurosci.* **22**, 389–442.

Sanes J. R., Marshall L. M. and McMahan U. J. (1978) Reinnervation of muscle fiber basal lamina after removal of myofibers. Differentiation of regenerating axons at original synaptic sites. *J. Cell Biol.* **78**, 176–198.

Sasahara R. M., Takahashi C. and Noda M. (1999) Involvement of the Sp1 site in ras-mediated downregulation of the RECK metastasis suppressor gene. *Biochem. Biophys. Res. Commun.* **264**, 668–675.

Sealock R., Wray B. E and Froehner S. C. (1984) Ultrastructural localization of the Mr 43,000 protein and the acetylcholine receptor in Torpedo postsynaptic membranes using monoclonal antibodies. *J. Cell Biol.* **98**, 2239–2244.

Takahashi C., Sheng Z., Horan T. P. *et al.* (1998) Regulation of matrix metalloproteinase-9 and inhibition of tumor invasion by the membrane-anchored glycoprotein RECK. *Proc. Natl Acad. Sci. USA* **95**, 13221–13226.

Takenaka K., Ishikawa S., Kawano Y. *et al.* (2004) Expression of a novel matrix metalloproteinase regulator, RECK, and its clinical significance in resected non-small cell lung cancer. *Eur. J. Cancer* **40**, 1617–1623.

Takeuchi T., Hisanaga M., Nagao M. *et al.* (2004) The membrane-anchored matrix metalloproteinase (MMP) regulator RECK in combination with MMP-9 serves as an informative prognostic indicator for colorectal cancer. *Clin Cancer Res.* **10**, 5572–5579.

Traub P (1995) Intermediate filaments and gene regulation. *Physiol. Chem. Phys. Med. NMR* **26**, 377–400.

Trinidad J. C., Fischbach G. D. and Cohen J. B. (2000) The Agrin/MuSK signaling pathway is spatially segregated from the neuregulin/ErbB receptor signaling pathway at the neuromuscular junction. *J. Neurosci.* **20**, 8762–8770.

Vaittinen S., Lukka R., Sahlgren C., Rantanen J., Hurme T., Lendahl U., Eriksson J. E. and Kalimo H. (1999) Specific and innervation-regulated expression of the intermediate filament protein nestin at neuromuscular and myotendinous junctions in skeletal muscle. *Am. J. Pathol.* **154**, 591–600.

VanSaun M., Herrera A. A. and Werle M. J. (2003) Structural alterations at the neuromuscular junctions of matrix metalloproteinase 3 null mutant mice. *J. Neurocytol.* **32**, 1129–1142.

Werb Z. (1997) ECM and cell surface proteolysis: regulating cellular ecology. *Cell* **91**, 439–442.

Yang X., Arber S., William C., Li L., Tanabe Y., Jessell T. M., Birchmeier C. and Burden S. J. (2001) Patterning of muscle acetylcholine receptor gene expression in the absence of motor innervation. *Neuron* **30**, 399–410.

